

**Supporting Information For**

**Solid-phase microextraction low temperature plasma mass spectrometry for the direct and  
rapid analysis of chemical warfare simulants in complex mixtures**

Morphy C. Dumlao, Laura E. Jeffress, J. Justin Gooding, William A. Donald\*

School of Chemistry, University of New South Wales, Sydney, New South Wales, 2052,

Australia

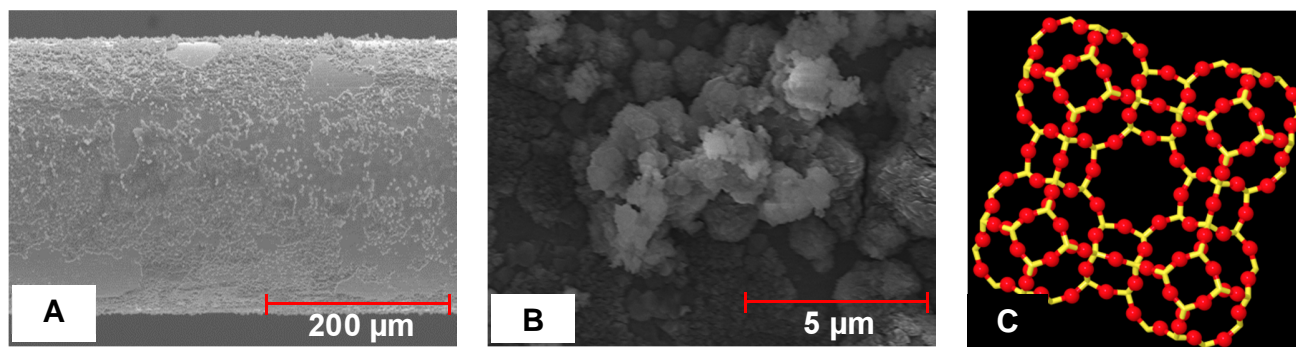


**Figure S1.** (A, B) Scanning electron microscope images of a Linde Type A coated stainless steel needle at two magnifications, and (C) the structure of LTA, where yellow nodes correspond to either Si or Al and O atoms are red. In LTA, the ratio of Al and Si are equal. Whereas the Si-centres are formally neutrally charged, the Al-centres are formally negatively charged. The zeolites contain extra-frameworks cations that balance the negatively charged framework that can be readily cation-exchanged.

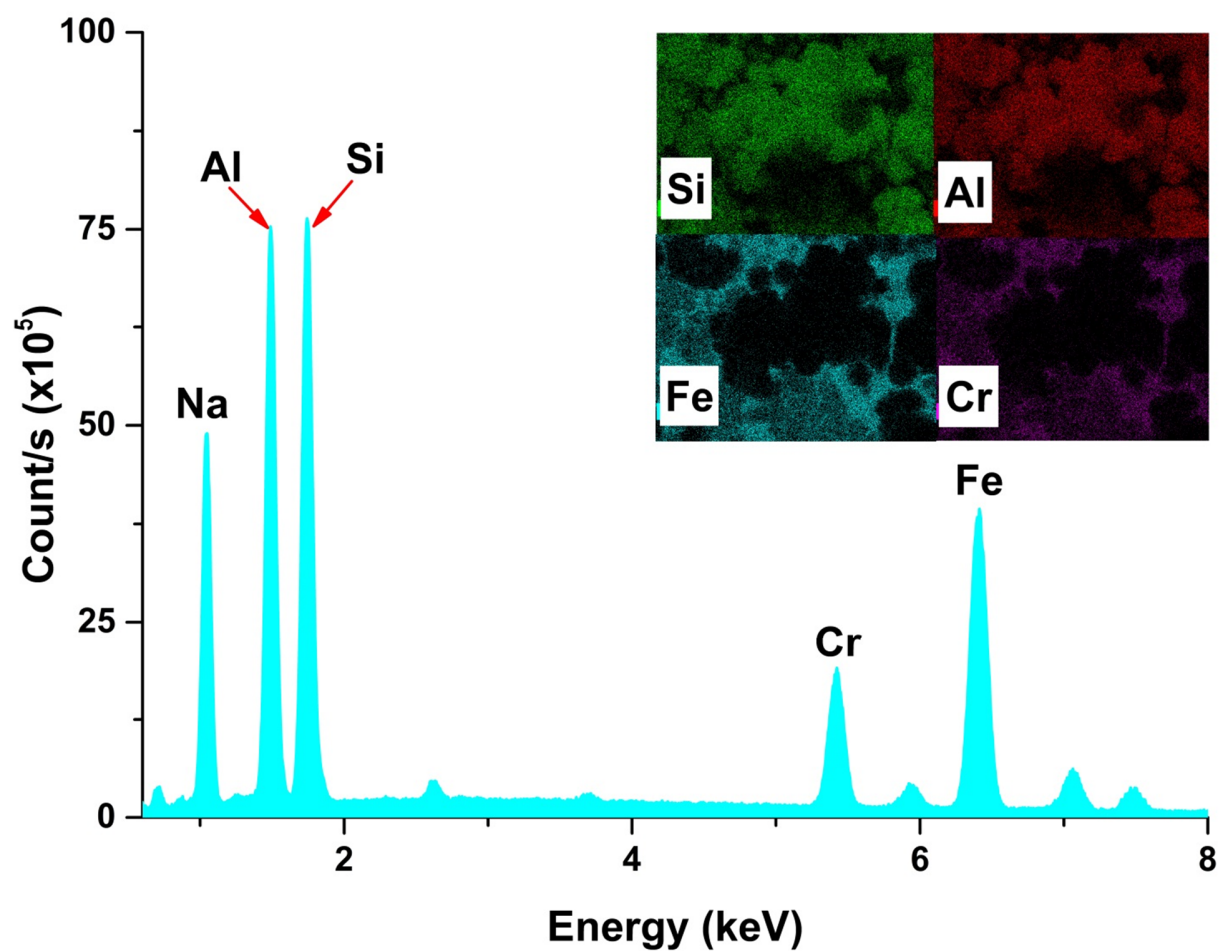


**Figure S2.** Energy dispersive SEM spectrum and image of a Linde Type A coated stainless steel needle, in which the Si/Al ratios ( $1.0 \pm 0.3$ ) were obtained. The presence of elements corresponding to the zeolite coating and the stainless steel substrate can be detected.

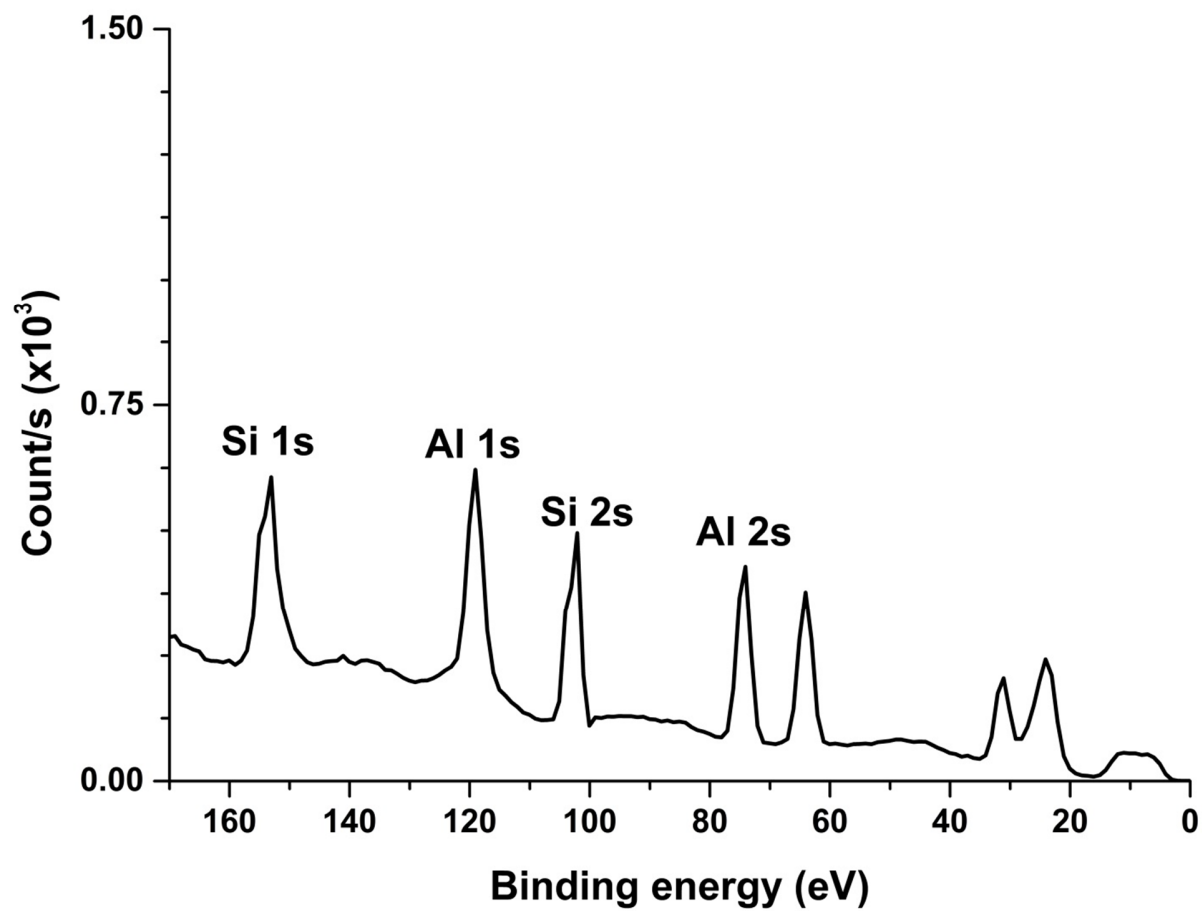


**Figure S3.** X-ray photoelectron spectrum of a Linde Type A coated stainless steel needle.

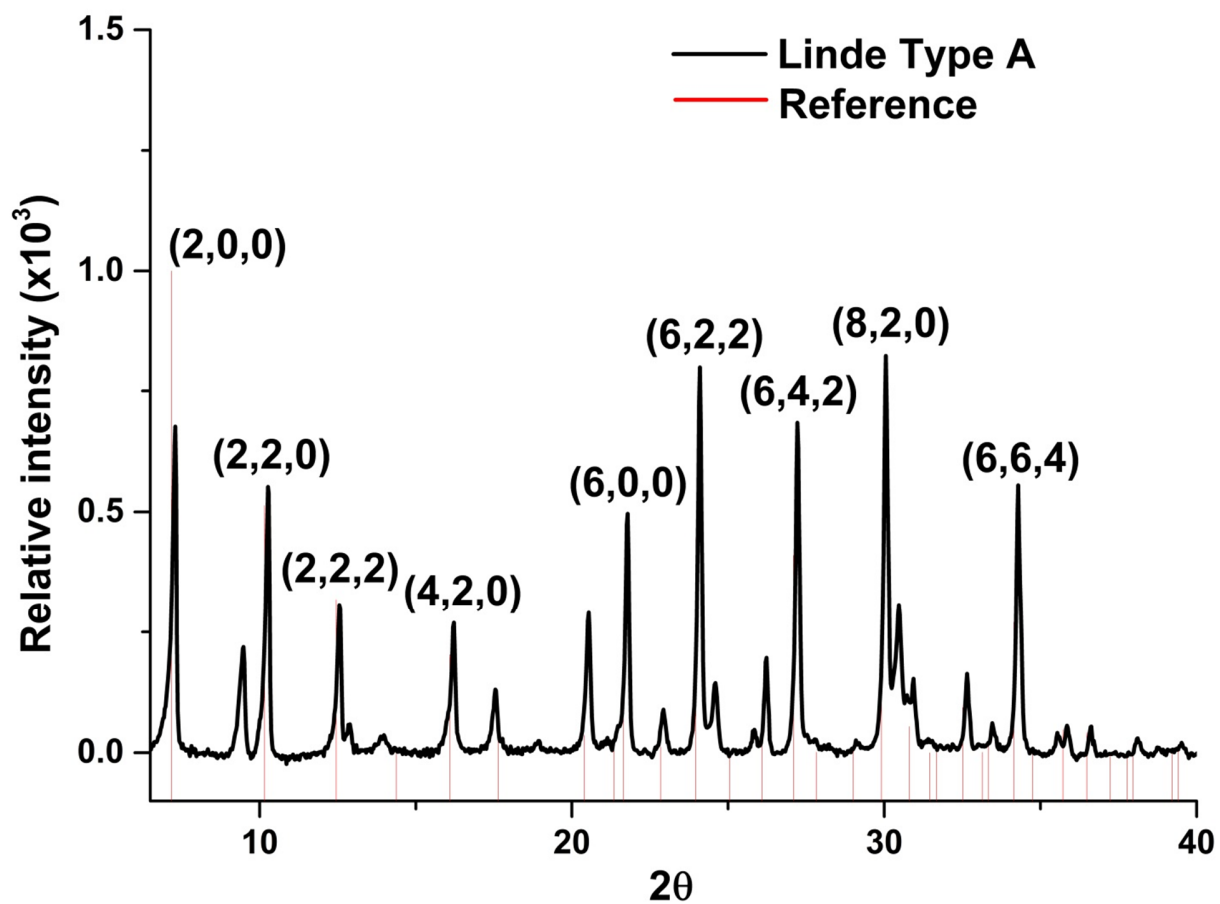


**Figure S4.** X-ray powder diffraction spectrum of Linde Type A zeolite powder (black) compared to the PANalytical X'Pert HighScore Plus (2015) library database pattern spectrum. Numbers in parentheses correspond to the Miller indices.

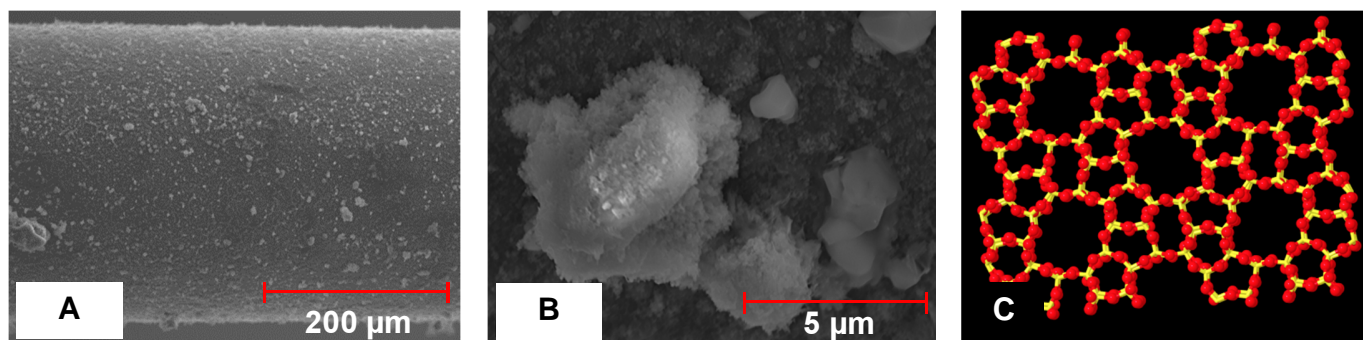


**Figure S5.** Scanning electron microscope images of a high alumina ZSM-5 coated needle at two different magnifications, and (C) the structure of ZSM-5, where yellow nodes correspond to either Si or Al and O atoms are red. In ZSM-5, the ratio of Al and Si are 13.3.

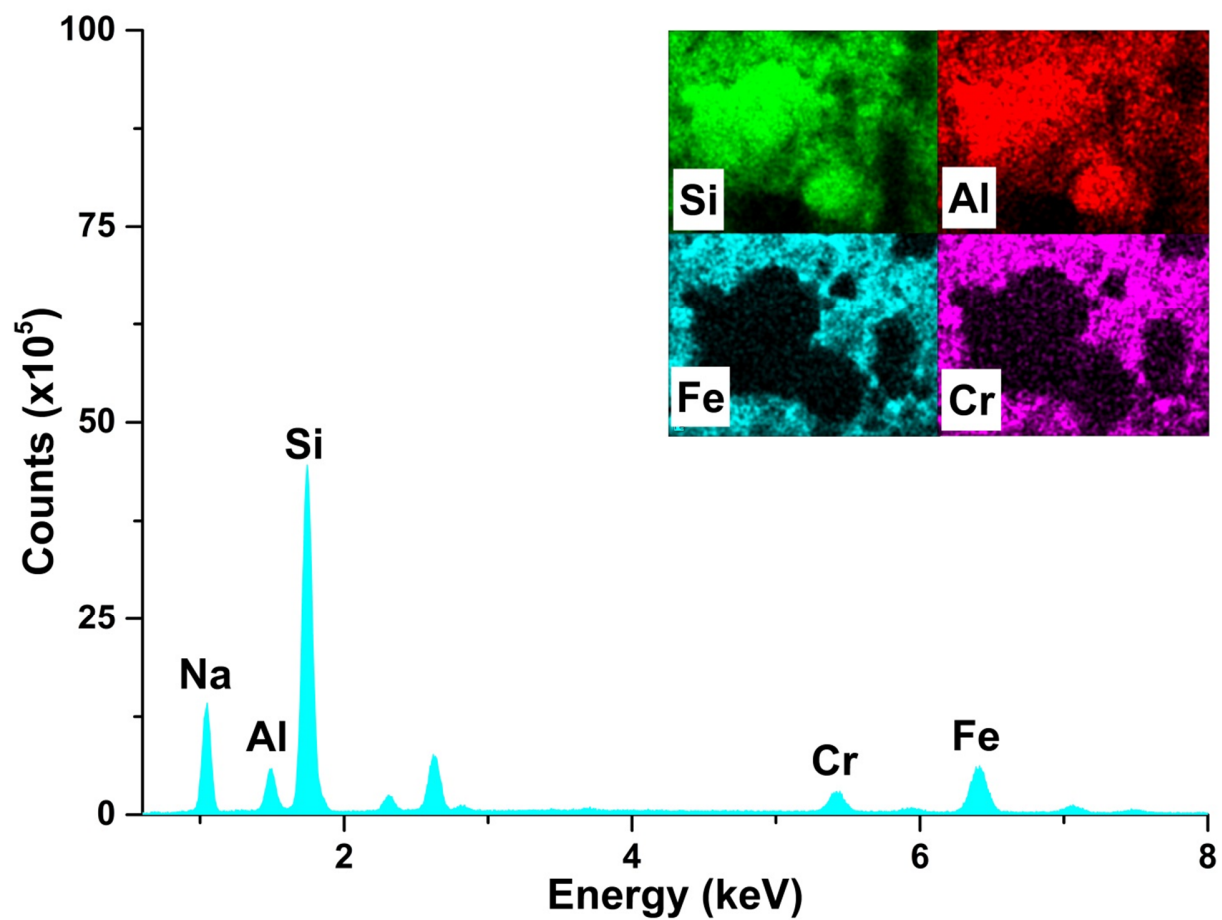


**Figure S6.** Energy dispersive SEM spectrum and image of a high alumina ZSM-5 coated stainless steel needle which the Si/Al ratios ( $13.6 \pm 0.3$ ) were obtained. The presence of elements corresponding to the zeolite coating and the stainless steel substrate can be detected.

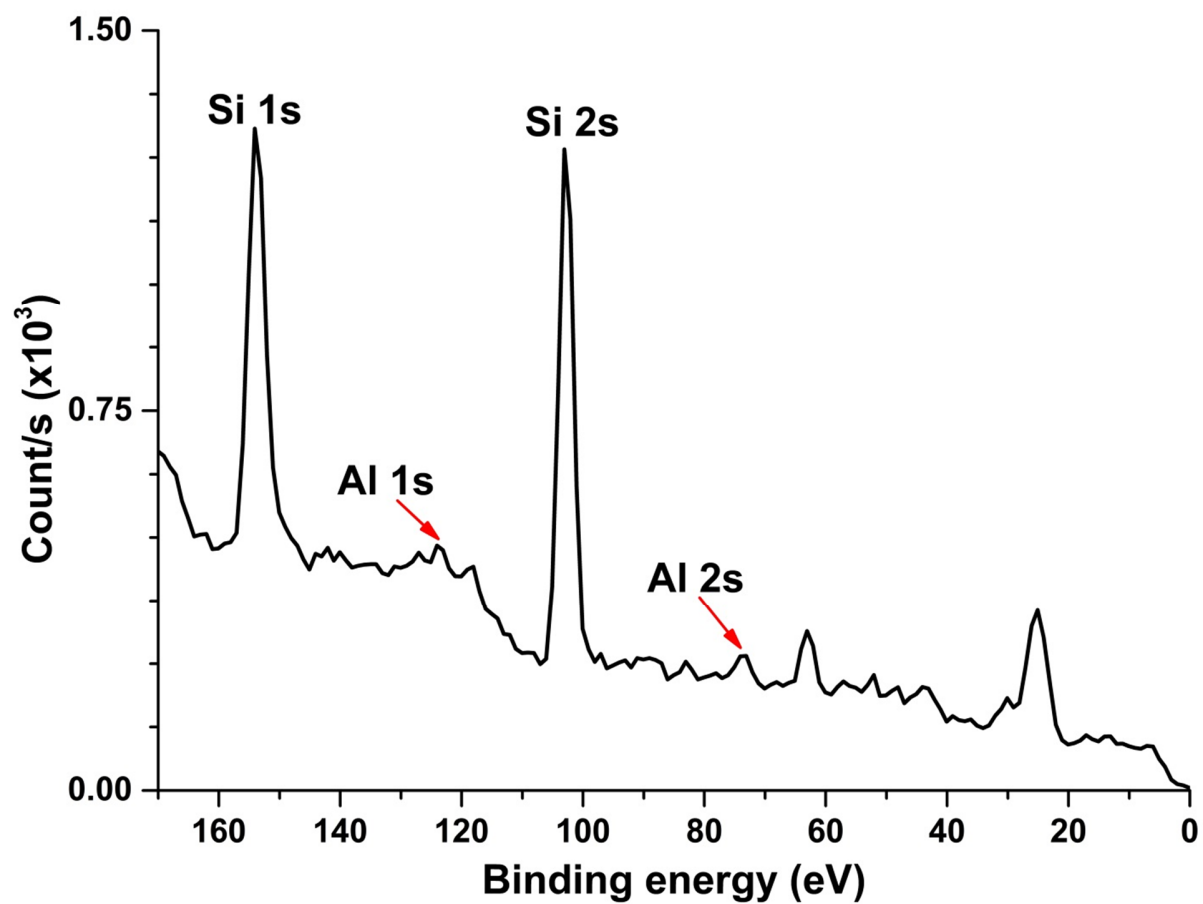
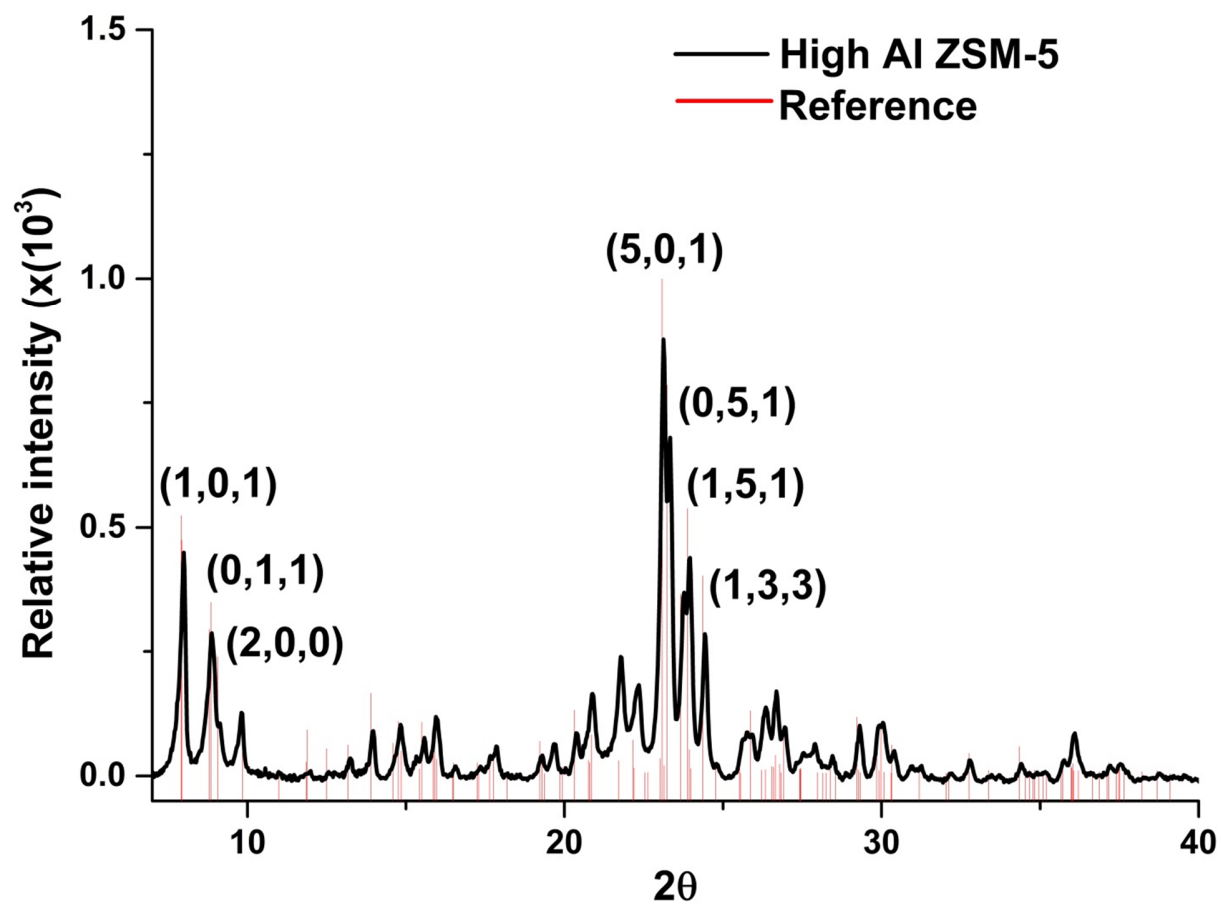
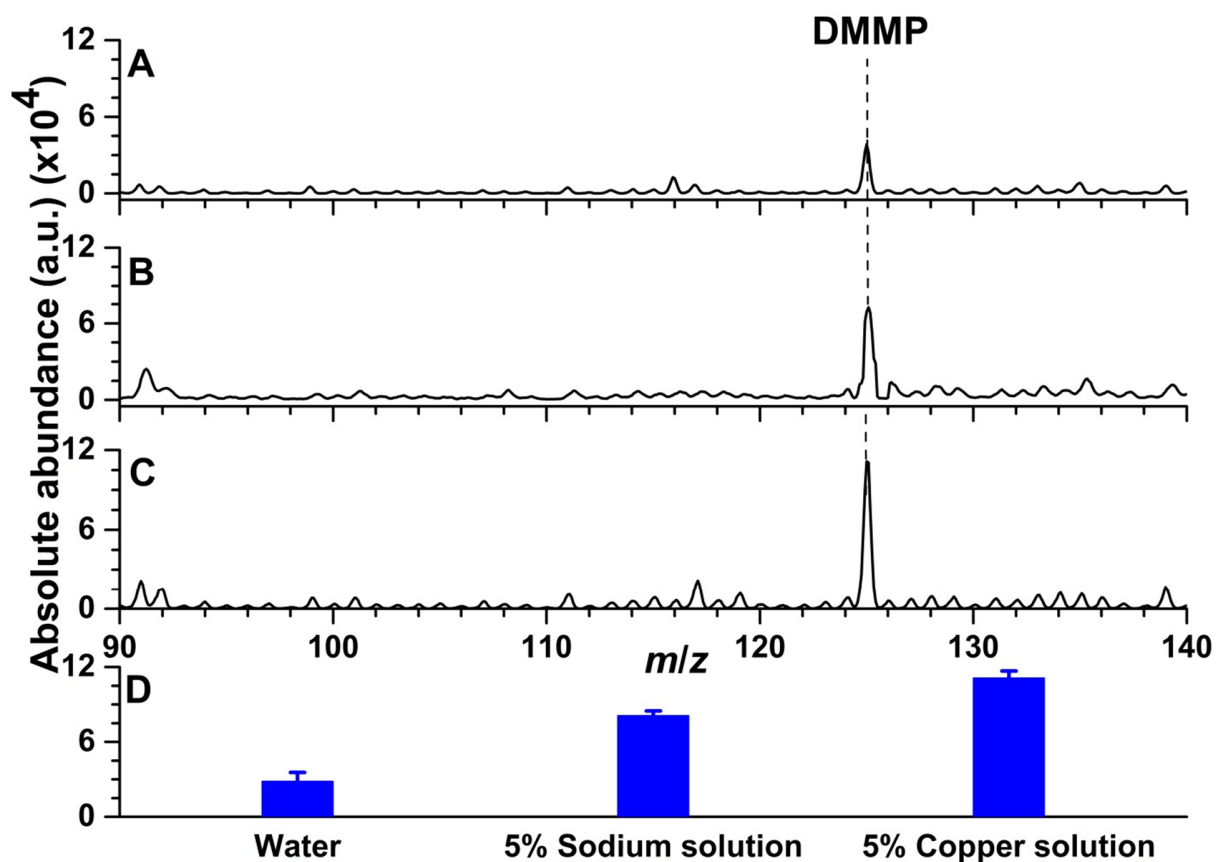


Figure S7. X-ray photoelectron spectrum of a high alumina ZSM-5 coated stainless steel needle.



**Figure S8.** X-ray powder diffraction spectrum of high alumina ZSM-5 zeolite powder (black) compared to the PANalytical X'Pert HighScore Plus (2015) library database pattern spectrum. Numbers in parentheses correspond to Miller indices.



**Figure S9.** Solid phase microextraction low temperature plasma mass spectra of an aqueous solution containing 100  $\mu\text{M}$  dimethyl methylphosphonate using an Linde Type A coated probe that was conditioned by immersion in a solution of (A) Milli-Q water, (B) 5% sodium chloride solution, and (C) 5% copper sulphate solution. (D) Bar graphs of the average and standard deviation of the ion abundances of protonated dimethyl methylphosphonate obtained for 5 replicate experiments.

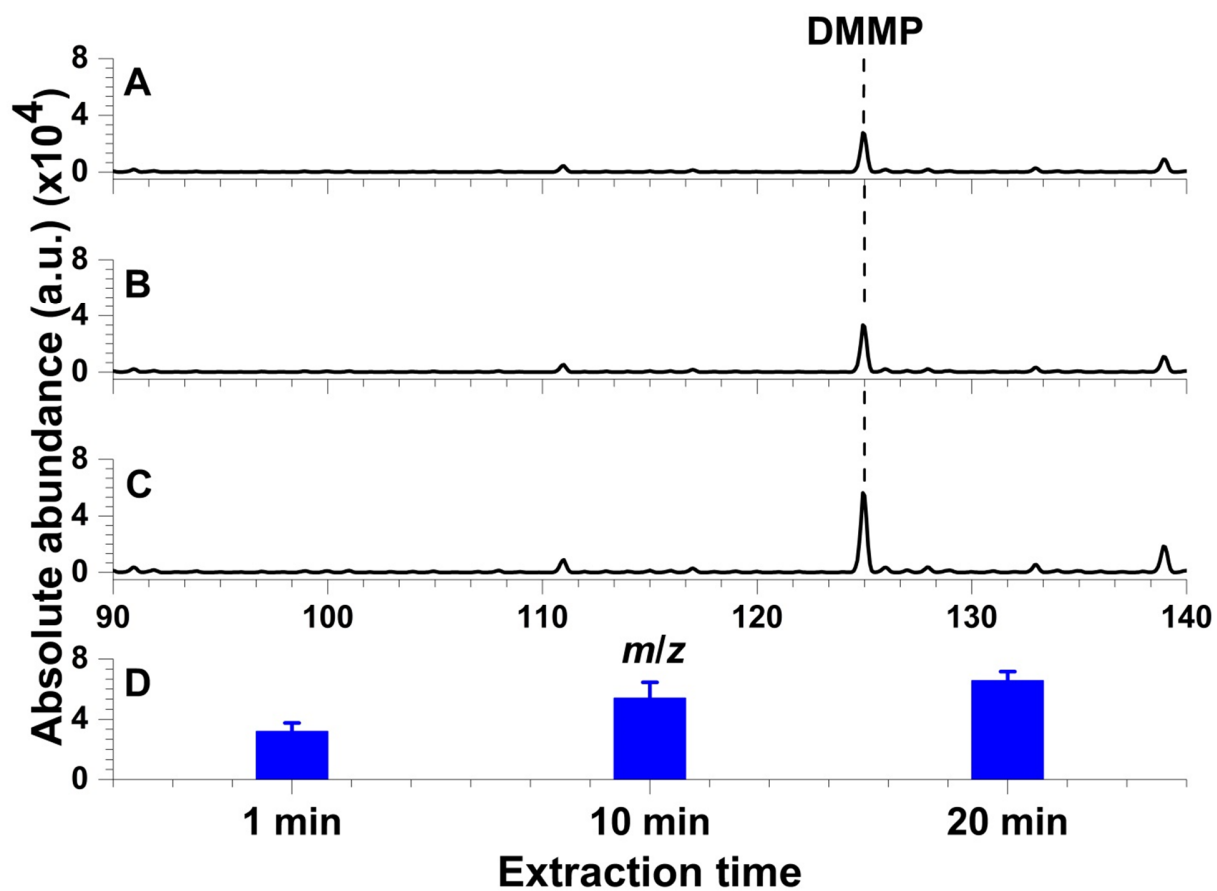


**Figure S10.** Solid phase microextraction low temperature plasma mass spectra of an aqueous solution containing 100  $\mu$ M dimethyl methyl phosphonate using different extraction time (**A**: 1 min, **B**: 10 mins, **C**: 20 mins). (**D**) Bar graphs of the average and standard deviation of the ion abundances of protonated DMMP obtained for 5 replicate experiments.

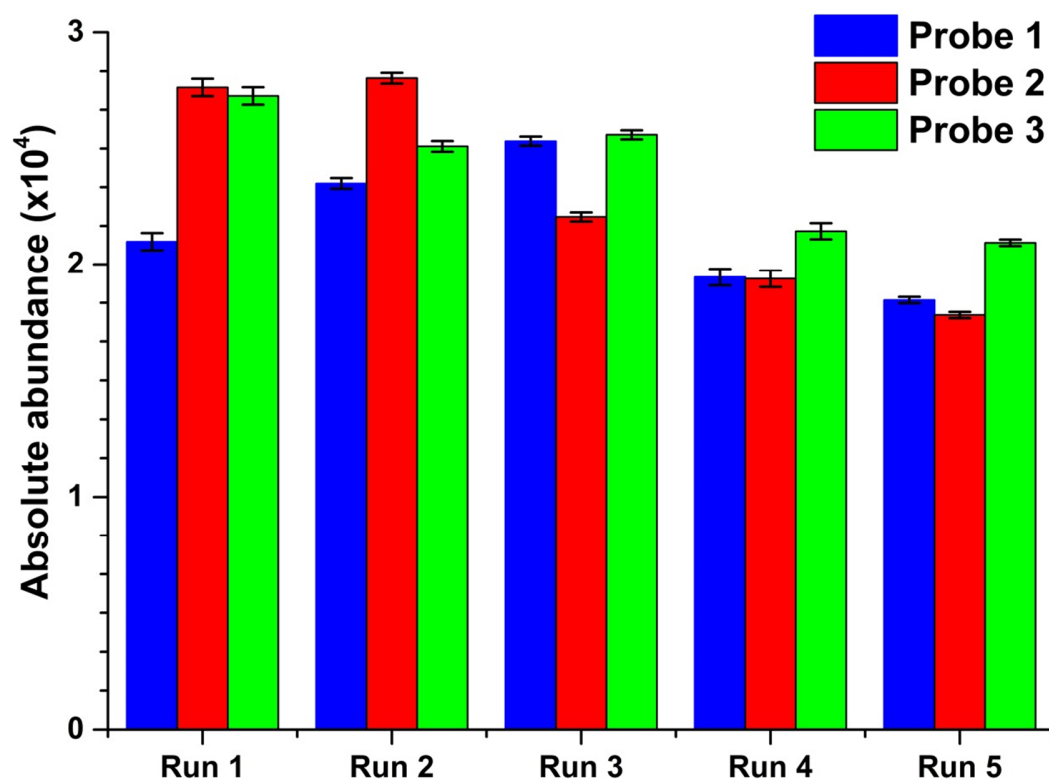


**Figure S11.** Bar graphs of the average Linde Type A solid phase microextraction low temperature plasma mass spectrometry ion abundances of protonated dimethyl methyl phosphonate obtained for three probes (synthesis replicates) upon five sequential measurements (sampling replicates).

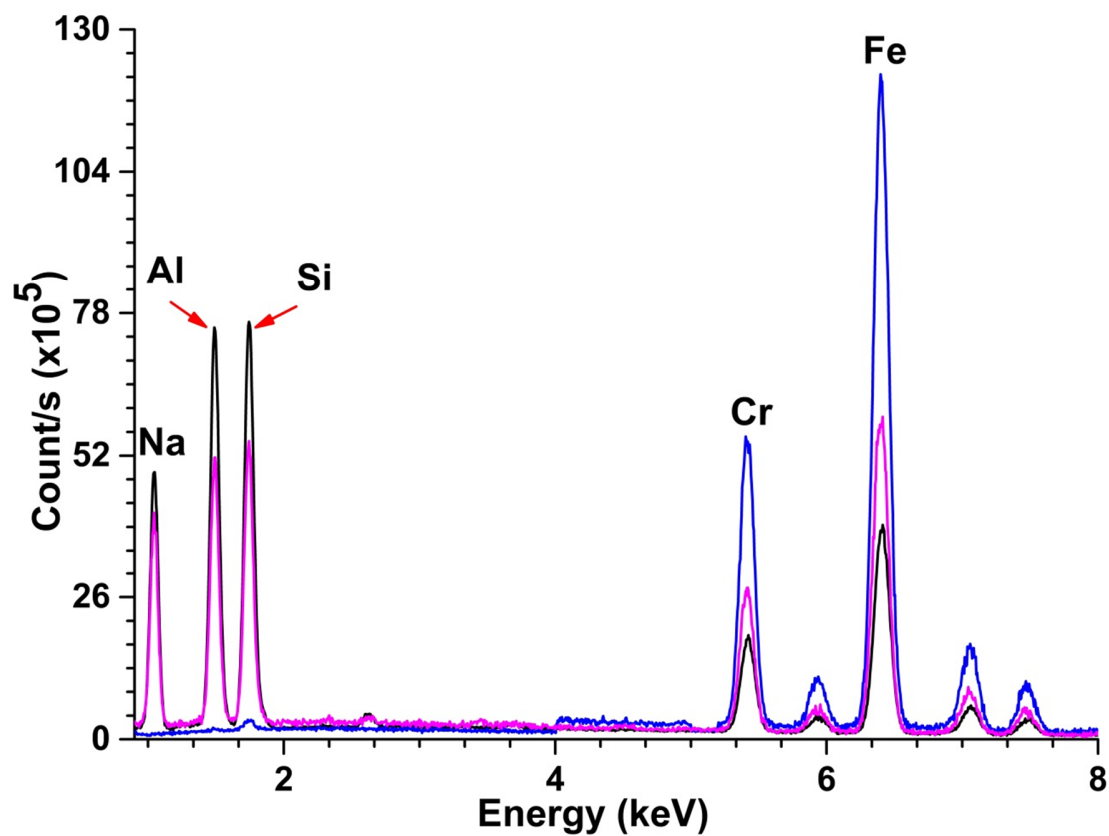


**Figure S12.** Energy dispersive SEM spectra of Linde Type A coating before (black) and after solid phase microextraction low temperature mass spectrometry sampling for 30 sequential times (magenta). The negative control spectrum of the uncoated stainless steel needle is shown in blue.